The Ellagitannin Metabolite Urolithin C is a Glucose-Dependent Regulator of Insulin Secretion through activation of L-type Calcium Channels

Morgane Bayle, Jeremie Neasta, Margherita Dall'Asta, Guillaume Gautheron, Anne Virsolvy, Jean-François Quignard, Estelle Youl, Richard Magous, Jean-François Guichou, Alan Crozier, et al.

The ellagitannin metabolite urolithin C is a glucose-dependent regulator of insulin secretion through activation of L-type calcium channels

Morgane Bayle[1] | Jérémie Neasta[2] | Margherita Dall'Asta[3] | Guillaume Gautheron[1] | Anne Virsolvy[4] | Jean-François Quignard[5] | Estelle Youl[1] | Richard Magous[1,2] | Jean-François Guichou[6] | Alan Crozier[7,8] | Daniele Del Rio[3] | Gérard Cros[1,2] | Catherine Oiry[1,2]

[1] IBMM, Univ Montpellier, CNRS, ENSCM, Montpellier, France

[2] Laboratoire de Pharmacologie, Faculté de Pharmacie, Univ Montpellier, Montpellier, France

[3] The Laboratory of Phytochemicals in Physiology, LS9 InterLab Group, Department of Food Science, University of Parma, Parma, Italy

[4] PhyMedExp, Univ Montpellier, CNRS, INSERM, Montpellier, France

[5] Université Bordeaux, INSERM U1045, Centre de Recherche Cardio-Thoracique de Bordeaux, Bordeaux, France

[6] CBS, Univ Montpellier, CNRS, INSERM, Montpellier, France

[7] Department of Nutrition, University of California, Davis, California

[8] School of Medicine, Dentistry and Nursing, University of Glasgow, Glasgow, UK

Correspondence
Professor Catherine Oiry, Institut des Biomolécules Max Mousseron (IBMM) UMR 5247, Faculté de Pharmacie, 15 Avenue Charles Flahault BP14491, 34093 Montpellier, Cedex 5, France.
Email: catherine.oiry-cuq@umontpellier.fr

Funding information
SATT AxLR; the Agence Nationale de la Recherche, Grant/Award Number: ANR-10-BINF-03-03

Background and Purpose: The pharmacology of polyphenol metabolites on beta-cell function is largely undetermined. We sought to identify polyphenol metabolites that enhance the insulin-secreting function of beta-cells and to explore the underlying mechanisms.

Experimental Approach: INS-1 beta-cells and rat isolated islets of Langerhans or perfused pancreas preparations were used for insulin secretion experiments. Molecular modelling, intracellular Ca^{2+} monitoring, and whole-cell patch-clamp recordings were used for mechanistic studies.

Key Results: Among a set of polyphenol metabolites, we found that exposure of INS-1 beta-cells to urolithins A and C enhanced glucose-stimulated insulin secretion. We further characterized the activity of urolithin C and its pharmacological mechanism. Urolithin C glucose-dependently enhanced insulin secretion in isolated islets of Langerhans and perfused pancreas preparations. In the latter, enhancement was reversible when glucose was lowered from a stimulating to a non-stimulating concentration. Molecular modelling suggested that urolithin C could dock into the $Ca_v1.2$ L-type Ca^{2+} channel. Calcium monitoring indicated that urolithin C had no effect on basal intracellular Ca^{2+} but enhanced depolarization-induced increase in intracellular Ca^{2+} in INS-1 cells and dispersed cells isolated from islets. Electrophysiology studies indicated that urolithin C dose-dependently enhanced the L-type Ca^{2+} current for levels of depolarization above threshold and shifted its voltage-dependent activation towards more negative potentials in INS-1 cells.

Conclusion and Implications: Urolithin C is a glucose-dependent activator of insulin secretion acting by facilitating L-type Ca^{2+} channel opening and Ca^{2+} influx into pancreatic beta-cells. Our work paves the way for the design of polyphenol metabolite-inspired compounds aimed at ameliorating beta-cell function.

1 | INTRODUCTION

Pancreatic beta cells play a key role in the control of blood glucose level by secreting insulin. Once transported into beta-cells, glucose undergoes a complex metabolic sequence that leads to elevation of intracellular ATP/ADP ratio. This in turn inhibits **ATP-sensitive K^+** channels (K_{ATP}) which causes membrane depolarization and thus the opening of **voltage-gated L-type Ca^{2+}** channels. The ensuing increase in intracellular $[Ca^{2+}]$ ($[Ca^{2+}]_i$), which is the primary mediator of the fusion of insulin-secretory granules with the plasma membrane, triggers insulin exocytosis (Rorsman & Ashcroft, 2018). Proteins involved in this series of events constitute druggable targets to overcome the deficit of glucose-induced insulin secretion which is a core feature of the pathogenesis and the evolution of Type 2 diabetes (Oh & Olefsky, 2016; Vetere, Choudhary, Burns, & Wagner, 2014). For instance, sulphonylureas bind to beta cell K_{ATP} channels and mediate their closing which in turn promotes insulin secretion in a way that is largely independent of glucose levels both in vitro and in vivo. The use of compounds that improve insulin secretion in a glucose-dependent manner is predicted to be a safer strategy to help achieve glycaemic goals due to lower risk of hypoglycaemia (Vetere et al., 2014). The development of such lead molecules is still an active area of research in order to provide more therapeutic options in the future as the number of Type 2 diabetic patients keeps growing (Zheng, Ley, & Hu, 2018).

In this context, plant polyphenols are likely good candidates since several of these well-known antioxidant compounds are now widely regarded as pharmacological agents that regulate target proteins and associated signalling pathways including in pancreatic beta cells (Dall'Asta et al., 2015; Goszcz, Duthie, Stewart, Leslie, & Megson, 2017; Oak et al., 2018; Saponara, Carosati, Mugnai, Sgaragli, & Fusi, 2011). The possibility of developing polyphenol-based therapeutics is further supported by studies reporting that a number of polyphenols elicit therapeutic-like effects at pharmacological micromolar concentrations in cells, tissues, and various animal models (Bai et al., 2017; Gu et al., 2017; Wright, 2013; Zhao et al., 2018). However and in contrast to the naturally occurring plant polyphenols, the bioactivity of their metabolite derivatives has more recently emerged and hence is still poorly characterized (Del Rio et al., 2013; Espín, Larrosa, García-Conesa, & Tomás-Barberán, 2013; Goszcz et al., 2017). In particular, the extensive metabolism of polyphenols in both the gastrointestinal tract and liver offers a collection of potential valuable compounds whose pharmacology on beta cell function is largely unknown.

In the present study, a screen of several polyphenol metabolites was undertaken using an insulin-secreting beta cell line in order to identify molecules improving glucose-induced insulin secretion. Further exploration of the insulin-secreting activity of one promising compound, namely, urolithin C, was then pursued using islets of Langerhans and isolated pancreas preparations. Finally, the pharmacological mechanism by which urolithin C enhanced insulin secretion was also investigated.

What is already known

- Pancreatic beta-cells play a key role in glycaemic control by secreting insulin.
- Plant polyphenols display pharmacological activity on cellular protein targets.

What this study adds

- The polyphenol metabolite urolithin C is a glucose-dependent activator of insulin secretion.
- Urolithin C modulates L-type Ca^{2+} channels currents and enhances Ca^{2+} influx.

What is the clinical significance

- Polyphenol metabolite-based compounds may be used to ameliorate pancreatic beta cell function in type 2 diabetes.

2 | METHODS

2.1 | Animals

All animal care and experimental proceduress complied with the Directive 2010/63/EU of the European Parliament and of the Council. Animal studies are reported in compliance with the ARRIVE guidelines (Kilkenny, Browne, Cuthill, Emerson, & Altman, 2010) and with the recommendations made by the *British Journal of Pharmacology*. Eight 9-week-old male Wistar rats (Crl:WI (Han), RRID:RGD_2308816, Charles River, France) weighing 280–300 g at the time of the experiments were used for pancreatic islets preparation and isolated perfused pancreas experiments. Wistar rats were previously used for the same purpose (Gross, Roye, Manteghetti, Hillaire-Buys, & Ribes, 1995; Youl et al., 2010). Animals were housed in groups of three per cage enriched with poplar heartwood modules in a temperature and humidity-controlled conventional animal facility under a 12-hr light: dark cycle and had water ad libitum. Animals used for pancreatic islets preparation had food ad libitum. Animals used for isolated perfused pancreas experiments were fed with 20 g·day^{-1} of standard diet.

2.2 | Insulin secretion experiments in INS-1 cells

INS-1 cells (RRID:CVCL_0352) were cultured in RPMI-1640 medium (containing 11 mmol·L^{-1} glucose) supplemented with 10% Fetal Calf Serum, 100 U·ml^{-1} penicillin, 100 µg·ml^{-1} streptomycin, 2 mmol·L^{-1} L-glutamine, 10 mmol·L^{-1} HEPES, 1 mmol·L^{-1} sodium pyruvate, and 50 µmol·L^{-1} 2-mercaptoethanol, in a humidified atmosphere (5% CO_2, 37°C). INS-1 cells were seeded in 24-well plates pre-coated with poly-L-lysine (4 x 10^5 cells per well) and cultured for 5 days before insulin secretion experiments. Glucotoxicity was induced by culturing cells for 48 hr in RPMI medium containing 25 mmol·L^{-1} glucose. Insulin

secretion was performed using static incubation experiments. Cells were washed with buffer 1 (123 mmol·L^{-1} NaCl, 5.4 mmol·L^{-1} KCl, 1.3 mmol·L^{-1} KH_2PO_4, 1.4 mmol·L^{-1} $MgSO_4$, 2.9 mmol·L^{-1} $CaCl_2$, 5 mmol·L^{-1} $NaHCO_3$, and 20 mmol·L^{-1} HEPES, pH 7.4) supplemented with 0.1% (*w*/*v*) BSA. Then, cells were incubated for 1 hr (5% CO_2, 37°C) in 500-µl buffer 1/BSA containing urolithin A, B, C, or D in the absence (non-stimulating condition; i.e., 1.4 mmol·L^{-1} glucose) or in the presence of secretagogue (8.3 mmol·L^{-1} glucose; 1.4 mmol·L^{-1} glucose + 10 nmol·L^{-1} **glibenclamide**); 8.3 mmol·L^{-1} glucose induces an intermediate and consistent enhancement of insulin secretion compared to basal glucose concentration (1.4 mmol·L^{-1}). Similarly to other studies, we used this intermediate concentration of glucose to avoid any saturation of the system that could mask a positive pharmacological effect on insulin secretion (Broca et al., 2009; Rebuffat et al., 2018; Youl et al., 2010). At the end of the 1-hr incubation period, supernatants were saved and stored at −20°C until insulin assay. The screening of polyphenol metabolites was carried out in the same condition in the presence of 8.3 mmol·L^{-1} of glucose only.

2.3 | Insulin secretion experiments in rat pancreatic islets

Rats were anaesthetized with isoflurane and killed by decapitation. The common bile duct was cannulated, and the pancreas was filled by injection of collagenase V solution (10 ml, 1 mg·ml^{-1}), excised, and digested at 37°C for 16 min. Islets were separated by Ficoll gradient and selected by hand-picking under a microscope. Then, islets were stabilized for 1 hr (5% CO_2, 37°C) in buffer 2 (120 mmol·L^{-1} NaCl, 4.7 mmol·L^{-1} KCl, 1.2 mmol·L^{-1} KH_2PO_4, 1.2 mmol·L^{-1} $MgSO_4$, 2.5 mmol·L^{-1} $CaCl_2$, 24 mmol·L^{-1} $NaHCO_3$, 0.1% BSA, pH 7.4) containing 2.8 mmol·L^{-1} glucose. Batches of five islets chosen at random were incubated for 1 hr at 37°C, in 1-ml buffer 2/BSA containing 2.8, 8.3, or 11.2 mmol·L^{-1} of glucose in the absence or presence of 20 µmol·L^{-1} urolithin C. At the end of the 1-hr incubation period, supernatants were saved and stored at −20°C until insulin assay.

2.4 | Insulin secretion experiments in rat isolated perfused pancreas

Rat was anaesthetized with pentobarbital (60 mg·kg^{-1}; i.p.), and pancreas was isolated from the neighbouring tissues as previously described (Gross et al., 1995). The pancreas was transferred into a thermostated (37°C) plastic chamber and was perfused through its own arterial system with buffer 3 (119 mmol·L^{-1} NaCl, 4.7 mmol·L^{-1} KCl, 1.2 mmol·L^{-1} KH_2PO_4, 1.2 mmol·L^{-1} $MgSO_4$, 2.5 mmol·L^{-1} $CaCl_2$, 23 mmol·L^{-1} $NaHCO_3$, 0.2% BSA, pH 7.4) containing 5 or 8.3 mmol·L^{-1} glucose depending on the experiment. Perfused medium was maintained at 37°C and continuously bubbled with 95% O_2/5% CO_2. Infusion pressure was adjusted to provide a pancreatic outflow rate of 2.5 ml·min^{-1} throughout the experiment. A 30-min equilibration period with 5 or 8.3 mmol·L^{-1} glucose was allowed before collecting the first sample. Then, depending on the topic of the experiment, each pancreas was perfused with 5 or 8.3 mmol·L^{-1} glucose, in the presence of 20 µmol·L^{-1} urolithin C or vehicle (DMSO). To determine the pancreatic flow rate, we measured the volume of each fraction collected for 1 min. Samples were stored at −20°C until insulin assay. Insulin release was calculated by multiplying insulin concentration by the flow rate.

2.5 | Insulin assays

Insulin quantification was performed using Cisbio Insulin assay kit according to the manufacturer's instructions.

2.6 | Comparative modelling and ligands docking in rat $Ca_v1.2$ channels

The rat $Ca_v1.2$ channel α_{1C} subunit sequence (P22002) was recovered from UniProt (UniProt, RRID:SCR_002380; http://www.uniprot.org/uniprot/). The search for homologous sequence and alignment were performed using @TOME-2 server (Pons & Labesse, 2009), and sequence of rabbit Oryctolagus cuniculus (P07293) was selected with a 77% of identity. Homology models of the rat $Ca_v1.2$ channel α_{1C} were generated using the electron microscopy structure of rabbit **Cav1.1** channel determined at 3.6-Å resolution as templates: Protein Data Bank accession no. 5GJV. Final models were built using Modeller 7.0 (MODELLER, RRID:SCR_008395; Webb & Sali, 2017) and evaluated using the dynamic evolutionary trace as implemented in ViTOusing @TOME-2 comparative option. The files for the ligands were generated with MarvinSketch 6.2.2 for the SMILES and with Frog2 server for the Sdf (Miteva, Guyon, & Tufféry, 2010). Docking simulation was performed using the server e-Drugs-3D (Pihan, Colliandre, Guichou, & Douguet, 2012) with a box of 100 Å × 100 Å × 100 Å to cover all the protein with no constraint. The pictures shown in Figures 6 and S4 were generated using PyMOL (PyMOL,RRID:SCR_000305) and MarvinSketch.

2.7 | Analysis of cytoplasmic Ca^{2+} variations in INS-1 cells and dispersed cells

Cytoplasmic Ca^{2+} variations ($[Ca^{2+}]_i$) were measured using the ratiometric fluorescent Ca^{2+} indicator Fura-2 as previously described (Bardy et al., 2013). Isolated cells were prepared by dispersion of islets with trypsin and plated on Lab-Tek® coverglass chambers (equivalent to 10 islets per chamber) in RPMI-1640 medium with 10% Fetal Calf Serum, 100 U·ml^{-1} penicillin, 100 µg·ml^{-1} streptomycin, and 2 mmol·L^{-1} L-glutamine. The experiments were performed on clusters of cells after 2 days of culture. INS-1 cells were cultured for 4 days in Lab-Tek® coverglass chambers before the experiment. Both cell types were incubated with 2.5 µmol·L^{-1} Fura-2AM plus 0.02% (v/v) Pluronic F-127 for 20 min then rinsed with buffer 2 and mounted on a microscope stage (Axiovert, Zeiss, Iena, Germany; 20× objective) during a 15-min waiting period for the de-esterification of Fura-2AM in the presence of either urolithin C (20 µmol·L^{-1}) or vehicle and with or without **nimodipine** (20 µmol·L^{-1}). Then, buffer 2 containing or not KCl (15 mmol·L^{-1}) and/or urolithin C and/or nimodipine was applied

directly on top of the imaged cells using a perfusion system. Images were captured digitally every 2 s with a cooled CCD camera (Photometrics, Roper scientific, Evry, France). Cells loaded with Fura-2AM were illuminated by excitation with a dual UV light source at 340 nm (Ca^{2+}-bound) and 380 nm (Ca^{2+}-free) using a λ DG-4 excitation system (Sutter Instrument Company, Novato, CA, USA). Fluorescence emission was measured at 510 nm and analysed (Metafluor software, Universal Imaging Corporation, Downingtown, PA). Changes in $[Ca^{2+}]_i$ were deduced from variations in the F340/F380 ratio after correction for background and dark currents.

2.8 | Electrophysiological recordings in INS-1 cells

Ca^{2+} channel currents were recorded using the whole-cell patch-clamp technique with a Biologic RK400 amplifier (Biologic, France). Data acquisition and analysis were performed using the pCLAMP system (Axon Instruments, Union City, CA, USA, pClamp, RRID:SCR_011323). Currents were recorded with patch pipettes of 2–5 MΩ. Capacitive transients were electronically compensated. Residual capacitive transient and linear leakage currents were subtracted using a four sub-pulse protocol. The extracellular solution contained 130 mmol−L^{-1} NaCl, 5.6 mmol·L^{-1} KCl, 1 mmol·L^{-1} $MgCl_2$, 1 mmol·L^{-1} glucose, 10 mmol·L^{-1} HEPES, 5 mmol·L^{-1} $BaCl_2$, adjusted to pH 7.4 with NaOH. The pipette solution contained 130 mmol·L^{-1} CsCl, 10 mmol·L^{-1} EGTA, 5 mmol·L^{-1} ATP Na_2, 2 mmol·L^{-1} $MgCl_2$, 10 mmol·L^{-1} HEPES, adjusted to pH 7.3 with CsOH. The holding potential was set at −80 mV, and depolarizing test pulses were applied as described. Compounds were applied to cells by pressure ejection from a glass pipette. To allow comparison of the magnitude of urolithin C effects in different experiments, the effect of urolithin C was quantified as percentage of response obtained with vehicle to control for unwanted sources of variation. All experiments were performed at room temperature.

2.9 | Randomization and blinding

Animals chosen at random from our weight-matched rat colonies were used either for perfused pancreas experiments or islet isolation. Urolithin C and control treatments were always performed in rat pancreatic islets originating from the same animal to reduce possible animal bias. Rat pancreatic islets were randomly assigned to different treatments. For insulin secretion experiments performed in INS-1 cells, treatment groups were randomly assigned to different wells within each 24-well plate. Unless otherwise stated, data analyses and experiments were not carried out under blind conditions. However, insulin secretion experiments were performed by different operators and yielded the same outcomes which reduced the need of blinding. In addition, statistical analyses were undertaken by another operator. All procedures except rat isolated perfused pancreas were previously standardized (Bardy et al., 2013; Youl et al., 2010) to improve reproducibility and lower the risk of technical bias.

2.10 | Data and statistical analysis

The data and statistical analysis comply with the recommendations of the *British Journal of Pharmacology* on experimental design and analysis in pharmacology (Curtis et al., 2018). All the data are expressed as mean ± SEM. Calculations of AUCs, correlations, and statistical analyses were performed using GraphPad Prism v6 software (GraphPad Prism, RRID:SCR_002798). Correlations were analysed by linear regression to compute Pearson correlation coefficient and the *P* value (two-tailed).

To ensure the reliability of singles values, technical triplicate and quintuplicate were used for insulin secretion experiments in INS-1 cells and rat pancreatic islets respectively. Image analyses of cytoplasmic Ca^{2+} in INS-1 cells and cells isolated from rat pancreatic islets were performed in triplicate. Group sizes "*n*" were designed to be equal and always represent the number of experimental independent repeats, each carried out with distinct biological preparations. For electrophysiological studies, calcium currents from one cell were recorded in each independent experiment. Group sizes suitable for each set of experiments were estimated to ensure adequate power and to detect a pre-specified effect based on the available literature, on pilot studies (rat isolated perfused pancreas), and on our previous reports (Bardy et al., 2013; Youl et al., 2010; Youl, Magous, Cros, & Oiry, 2014). Group sizes were set at $n \geq 5$ except otherwise stated. Depending on the design of the experiment, data were analysed with two-tailed unpaired *t*-test, one-way or two-way ANOVA. The Brown-Forsythe's test was used to assess equality of variances. When ANOVA achieved the necessary level of statistical significance ($P < .05$) and when no significant variance inhomogeneity was detected, Holm–Sidak multiple comparisons test was used to assign significance to the comparisons between groups. The limit of statistical significance was set at $P < .05$.

2.11 | Materials

Poplar heartwood modules for cage enrichment and Lignocel® Select Fine for bedding were from Safe. RPMI-1640 medium (#12-167F) was purchased from Lonza (Levallois Perret, France). Fetal Calf Serum was purchased from Eurobio (Les Ulis, France). Chemical reagents used for buffer preparation, collagenase V, glibenclamide, nimodipine, BSA, DMSO, Ficoll, trypsin, penicillin, streptomycin, poly-L-lysine, L-glutamine, phloroglucinol, protocatechuic acid, 4-hydroxybenzoic acid, 3,4-dihydroxyphenylacetic acid, caffeic acid, dihydrocaffeic acid, ferulic acid, dihydroferulic acid, 4′-hydroxyphenylacetic acid, pyrogallol, tyrosol, 4′-hydroxyhippuric acid, 3-(4′-hydroxyphenyl)lactic acid, 3-hydroxyphenylacetic acid, 4′-hydroxyphenylacetic acid, pyrocatechol, 4′-hydroxymandelic acid, and ellagic acid were obtained from Sigma-Aldrich (St. Louis, MO, USA). Quercetin-3-glucuronide, kaempferol-3-glucuronide, 3-*O*-methylgallic acid, 4-*O*-methylgallic acid, and homovanillic acid were purchased from Extrasynthese (Genay, France) and 3-(3′-hydroxyphenyl)propionic acid from Fluorochem (Hadfield, UK). Feruloylglycine and isoferuloylglycine were provided by Alan Crozier (Stalmach et al., 2009). Urolithins A, B, C, and D were obtained from Dalton Pharma Services (Toronto, ON, Canada).

Insulin quantification was determined using Cisbio Insulin assay kit (Cisbio International, Bagnols-sur-Cèze, France). Fura-2AM was purchased from TEF labs (Austin, TX, USA). Pluronic F-127 was purchased from Molecular Probes (Invitrogen, Cergy-Pontoise, France). Stock solutions of urolithins were dissolved at 20 mmol·L^{-1} in DMSO and stored at −20°C. Control treatments were always performed using the same amount of vehicle (DMSO). The final concentration of DMSO did not exceed 0.1% (*v*/v) and did not affect insulin secretion or Ca^{2+} measurements.

2.12 | Nomenclature of targets and ligands

Key protein targets and ligands in this article are hyperlinked to corresponding entries in http://www.guidetopharmacology.org, the common portal for data from the IUPHAR/BPS Guide to PHARMACOLOGY (Harding et al., 2018), and are permanently archived in the Concise Guide to PHARMACOLOGY 2017/18 (Alexander, Fabbro et al., 2017; Alexander, Striessnig et al., 2017).

3 | RESULTS

3.1 | Effects of a set of polyphenol metabolites on glucose-induced insulin secretion

Several metabolites originating from different classes of polyphenols were selected on the basis of previous studies reporting pharmacological activities in different biological systems (Del Rio et al., 2013; Giorgio et al., 2015; Tognolini et al., 2012; Table S1). These metabolites are produced by the transformation of polyphenols either by

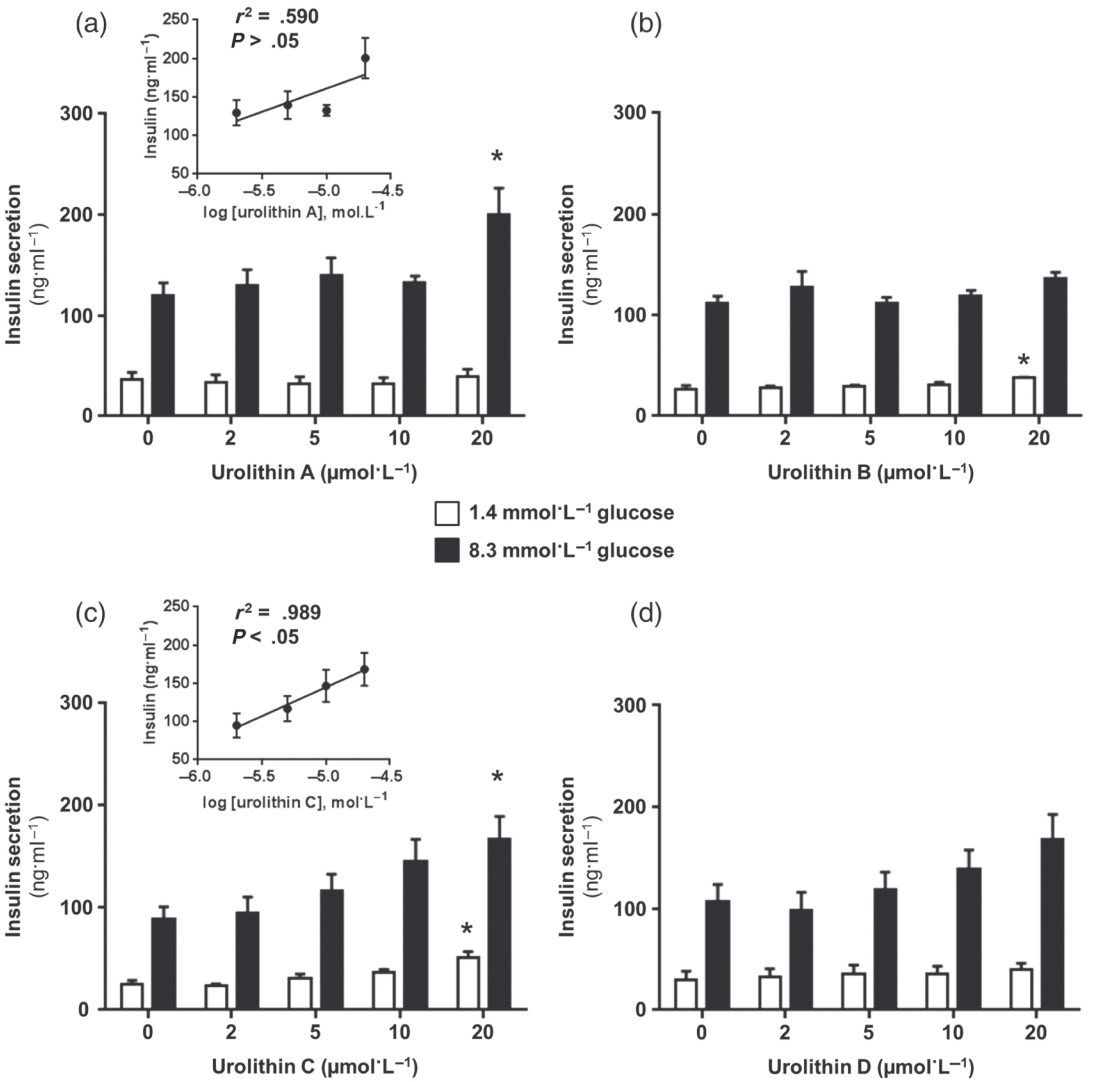

FIGURE 1 Effects of urolithins A, B, C, and D on basal and glucose-induced insulin secretion in INS-1 cells. The effects of increasing concentrations (2–20 µmol·L^{-1}) of (a) urolithin A, (b) urolithin B, (c) urolithin C, and (d) urolithin D in INS-1 cells were determined under basal non-stimulating (1.4 mmol·L^{-1} glucose) or 8.3 mmol·L^{-1} glucose-stimulated conditions. Inserts depict the correlation between insulin secretion and the log of urolithin concentration. Under non-stimulating glucose condition, there was a significant effect of the treatment for urolithin B and C. Under 8.3 mmol·L^{-1} glucose-stimulated condition, there was a significant effect of the treatment for urolithins A and C. *P < .05, significantly different from 0 µmol·L^{-1} urolithin, one-way ANOVA with Holm–Sidak test, n = 5

phase II metabolism or through the interaction with the human gut microbiota (Rodriguez-Mateos et al., 2014; Williamson, Kay, & Crozier, 2018). To estimate their activity on the insulin-secreting function of beta cell, INS-1 cells were exposed to these compounds at 2 and 20 μmol·L^{-1} for 1 hr under 8.3 mmol·L^{-1} of glucose-stimulated condition and insulin secretion was quantified. This intermediate stimulating concentration of glucose is appropriate to examine the potential stimulatory effect of a compound essentially to avoid any possible saturation of the system that could mask a pharmacological action (Broca et al., 2009; Jamen, Puech, Bockaert, Brabet, & Bertrand, 2002; Peyot et al., 2009; Rebuffat et al., 2018; Youl et al., 2010). A ~1.5-fold increase in glucose-induced insulin secretion was used as a cut-off to identify potential activators. As shown in Table S1, these exploratory data led to the identification of urolithins A, B, C, and D (see Figure S1 for chemical structures) as potential activators of glucose-induced insulin secretion when used at 20 μmol·L^{-1}. Therefore, we further examined the effects of these four compounds on insulin secretion.

3.2 | Effects of urolithins A, B, C, and D on insulin secretion in INS-1 cells

Concentration–response relationships of urolithin A, B, C, or D (2, 5, 10, and 20 μmol·L^{-1}) were first carried out under non-stimulating (1.4 mmol·L^{-1} glucose) or intermediate-stimulating (8.3 mmol·L^{-1} glucose) concentrations (Figure 1). Under non-stimulating condition, urolithins B and C increased insulin secretion at the highest concentration tested (20 μmol·L^{-1}). Under 8.3 mmol·L^{-1} glucose-stimulated condition, 20 μmol·L^{-1} urolithins B and D did not significantly enhance glucose-induced insulin secretion (Figure 1b,d). In contrast, 20 μmol·L^{-1} urolithins A and C enhanced insulin secretion. In addition, when insulin secretion was plotted against the log of urolithin concentration, a significant correlation was observed for urolithin C (r^2 = .989) but not for urolithin A (r^2 = .590; Figure 1a,c). This suggested that urolithin C was more potent than urolithin A and that its effect on glucose-induced insulin secretion was concentration dependent within the range of concentrations tested. Therefore, we examined whether higher concentrations of urolithin C (20–200 μmol·L^{-1}) also modulated glucose-induced insulin secretion. We found that the effect of urolithin C peaked at 100 μmol·L^{-1} and declined under control value at 200 μmol·L^{-1} (Figure S2).

Next, we aimed at determining whether urolithins were also able to modulate insulin secretion induced by insulinotropic drugs and in particular the non-glucose-dependent sulfonylurea glibenclamide. Urolithins A, B, C, and D at 2, 5, 10, and 20 μmol·L^{-1} were tested in the presence of 1.4 mmol·L^{-1} of glucose + 10 nmol·L^{-1} of glibenclamide (Figure 2). As expected, glibenclamide induced an increase in insulin secretion. Urolithins A, C, and D enhanced glibenclamide-stimulated insulin secretion when tested at 20 μmol·L^{-1}. A significant correlation between insulin secretion and the log of urolithin concentration was observed for both urolithins A (r^2 = .941) and C (r^2 = .959). In summary, our data suggest that urolithins A and C (20 μmol·L^{-1}) displayed the greatest capacity to enhance glucose- and glibenclamide-stimulated insulin secretion.

3.3 | Effects of urolithins A, B, C, and D in glucotoxicity-induced dysfunctional INS-1 cells

The capacity of urolithins to promote insulin secretion in dysfunctional INS-1 cells was investigated (Figure 3). Dysfunction was induced by culturing INS-1 cells in 25 mmol·L^{-1} glucose for 48 hr. As expected, glucotoxicity strongly impaired glucose-induced insulin secretion (Quinault et al., 2016). As shown in Figure 3, urolithins A and C (20 μmol·L^{-1}) retained some capacity to stimulate insulin secretion in dysfunctional INS-1 cells while urolithins B and D were inactive. These data indicate that urolithins A and C partly restored insulin secretion in INS-1 cells that were unresponsive to glucose following glucotoxic insult.

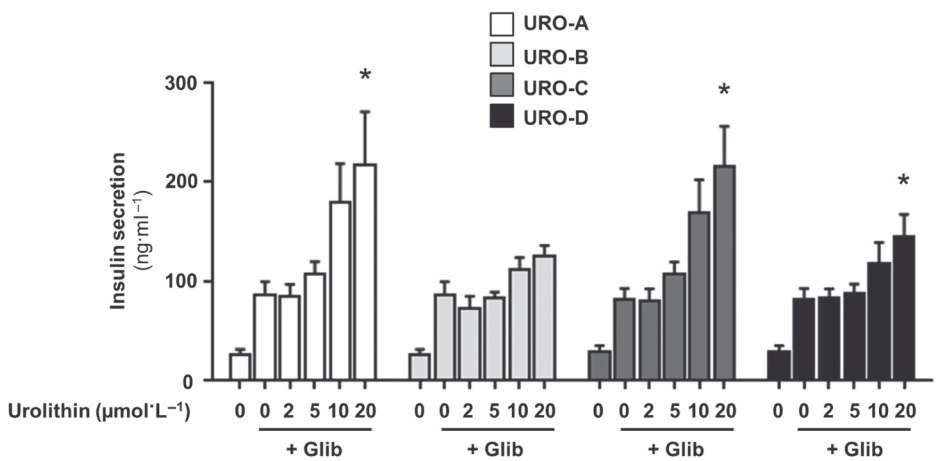

FIGURE 2 Effects of urolithins A, B, C, and D on insulin secretion induced by glibenclamide in INS-1 cells. The effects of increasing concentrations (2–20 μmol·L^{-1}) of urolithin A (URO-A), urolithin B (URO-B), urolithin C (URO-C), and urolithin D (URO-D) were determined in the presence of 1.4 mmol·L^{-1} glucose + 10 nmol·L^{-1} glibenclamide (+Glib). There was a significant effect of the treatment for urolithins A, C, and D. *P < .05, significantly different from 0 μmol·L^{-1} urolithin in the presence of glibenclamide; one-way ANOVA with Holm–Sidak test, n = 5

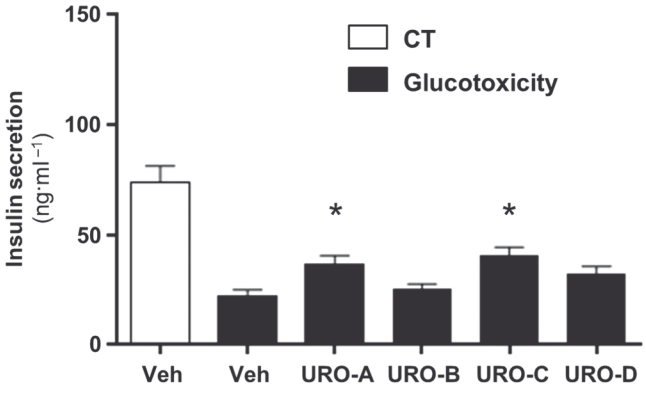

FIGURE 3 Effects of urolithins A, B, C, and D on insulin secretion in dysfunctional INS-1 cells. INS-1 cells were cultured in a control medium (CT) or in a medium containing 25 mmol·L^{-1} glucose for 48 hr (glucotoxicity). Then, cells were incubated with 8.3 mmol·L^{-1} glucose, in the absence (Veh) or in the presence of 20 μmol·L^{-1} urolithin A (URO-A), urolithin B (URO-B), urolithin C (URO-C), or urolithin D (URO-D). There was a significant effect of the treatment under glucotoxicity for urolithins A and C. *P < .05, significantly different from Veh under glucotoxicity, one-way ANOVA with Holm–Sidak test, n = 7

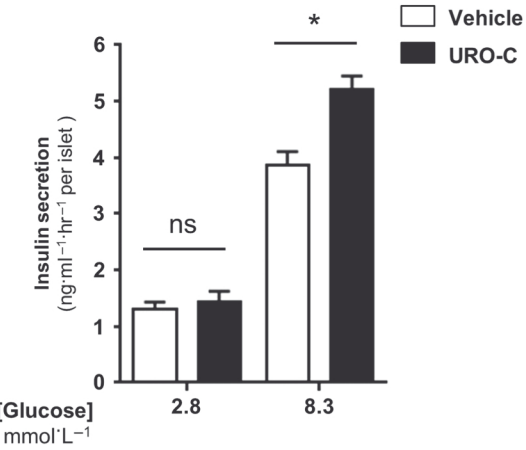

FIGURE 4 Effect of urolithin C on basal and glucose-induced insulin secretion in rat pancreatic islets. Rat pancreatic islets were incubated in the absence (Vehicle) or in the presence of 20 μmol·L^{-1} urolithin C (URO-C) under basal non-stimulating (2.8 mmol·L^{-1} glucose) or 8.3 mmol·L^{-1} glucose-stimulated conditions. There was an effect of the glucose and urolithin C as well as an interaction between both factors. *P < .05, significantly different as indicated, ns, non-significant; two-way ANOVA with Holm–Sidak test, n = 6

In summary, the data obtained in INS-1 cells indicated that urolithins A and C were the most active compounds on the basis of their capacity to promote insulin secretion under normal or dysfunctional conditions. As urolithin C appeared to be more potent than urolithin A and because its effect was concentration dependent on both glucose- or glibenclamide-induced insulin secretion, we decided to further explore its pharmacological properties and mechanism of action.

3.4 | Effects of urolithin C on insulin secretion in rat isolated islets of Langerhans and isolated perfused pancreas

Isolated rat pancreatic islets were incubated with urolithin C (20 μmol·L^{-1}) in the presence of either a non-stimulating (2.8 mmol·L^{-1}) or a stimulating (8.3 mmol·L^{-1}) glucose concentration (Figure 4). We observed that urolithin C increased insulin secretion in the presence of 8.3 mmol·L^{-1} but not 2.8 mmol·L^{-1} glucose. We also confirmed the stimulating effect of urolithin C under higher concentration of glucose (11.2 mmol·L^{-1}; Figure S3). Insulin secreting capacity of urolithin C was further characterized in a dynamic model, the isolated perfused rat pancreas (Figure 5). In a first set of experiments, insulin secretion of isolated pancreas was stabilized by infusing 8.3 mmol·L^{-1} glucose before urolithin C (20 μmol·L^{-1}) was infused under the same glucose concentration. Urolithin C enhanced glucose-induced insulin secretion (Figure 5a); its stimulatory effect occurred rapidly as insulin secretion peaked within minutes. This enhancement was sustained throughout the 30-min urolithin C infusion (from 17 to 47 min). The corresponding AUCs determined in the absence and presence of urolithin C were significantly different (see insert Figure 5a). In contrast, when 20 μmol·L^{-1} urolithin C was infused under a non-stimulating concentration of glucose (5 mmol·L^{-1}), it did not induce any insulin secretion (Figure 5b). In order to further explore the glucose dependency of the effect of urolithin C, the pancreas was infused with 20 μmol·L^{-1} of urolithin C in the presence of 8.3 mmol·L^{-1} of glucose for 30 min, before reducing the glucose concentration to 5 mmol·L^{-1}, while maintaining urolithin C at 20 μmol·L^{-1}. As shown in Figure 5c,d, reduction of the glucose concentration overlapped with a concomitant decrease in insulin secretion, further illustrating the glucose dependency of the insulin secreting activity of urolithin C. In summary, these findings further suggest that urolithin C is a glucose-dependent regulator of insulin secretion.

3.5 | Role of L-type Ca^{2+} channels in the mechanism of action of urolithin C

Calcium influx through L-type Ca^{2+} channels is crucial for glucose-induced insulin secretion (Rorsman & Ashcroft, 2018). Therefore, we sought to examine their involvement in the mechanism of action of urolithin C.

Firstly, the possible interaction of urolithin C with the rat $Ca_v1.2$ channel protein was evaluated by molecular in silico docking simulation. To this end, the homology model of the central pore of the rat α1c subunit was reconstructed using the central pore of the rabbit α1s, sharing 77% of sequence identity. To validate the model, we made docking simulations with three L-type Ca^{2+} channel reference molecules: **verapamil** and nimodipine (two Ca^{2+} channel inhibitors; Figure S4A,B) and **(-)-(S)-Bay K8644** (a Ca^{2+} channel agonist, Figure S4C). As previously described (Fusi, Spiga, Trezza, Sgaragli, & Saponara, 2017), we observed that verapamil and Bay K8644 bind into two pocket regions within close proximity. In addition, the simulation of verapamil and nimodipine dockings were compatible with the X-ray structures of Br-verapamil and nimodipine bound to the bacterial

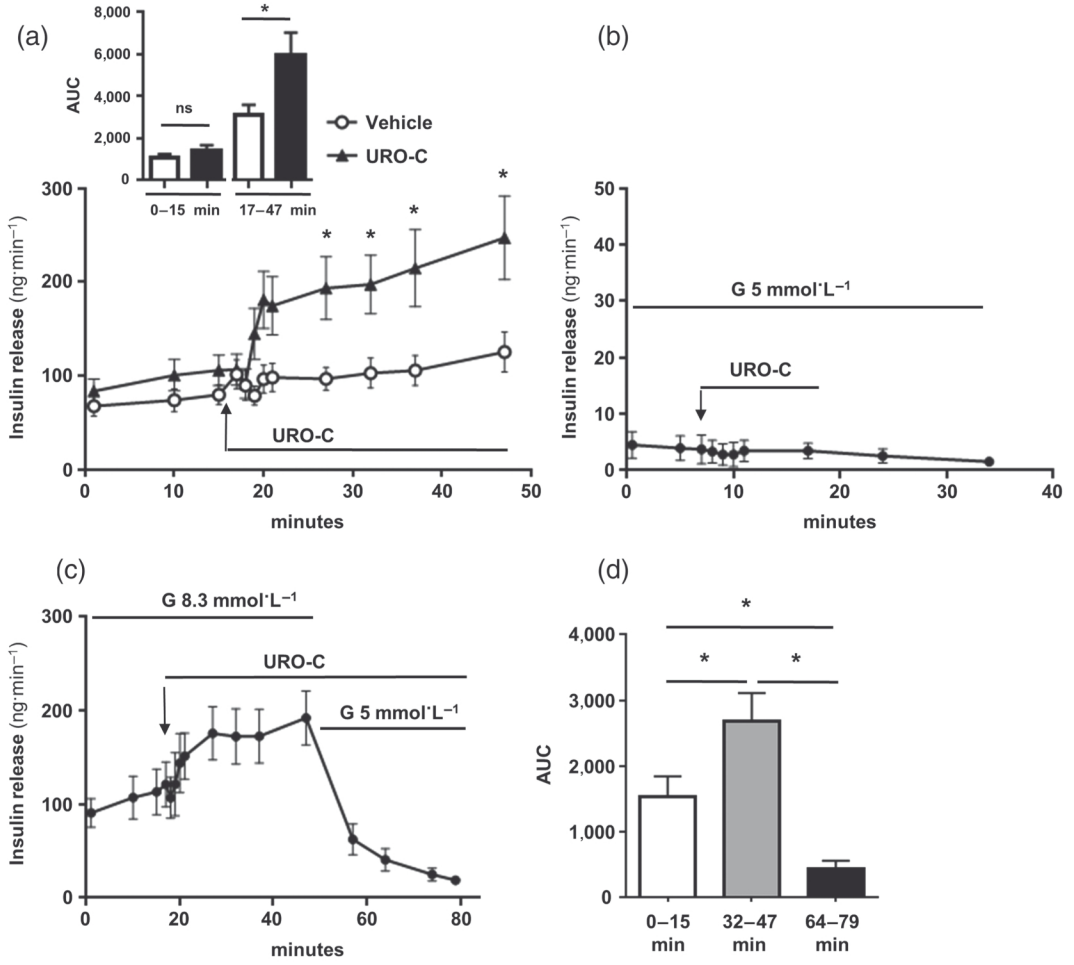

FIGURE 5 Effects of urolithin C on insulin release in rat isolated perfused pancreas. (a) A whole pancreas was isolated prior to perfusion with 8.3 mmol·L^{-1} glucose throughout the experiment. After the addition of urolithin C or vehicle (from 17 to 47 min) there was an effect of the treatment and an interaction between time and treatment. *P < .05 significantly different from vehicle; two-way ANOVA with repeated measures and Holm–Sidak test. Insert depicts the mean AUC of insulin release before (0–15 min) and after (17–47 min) addition of urolithin C or vehicle. *P < .05, significantly different as indicated, ns, non-significant; t-test; n = 5. (b) A pancreas was perfused with 5 mmol·L^{-1} of glucose throughout the experiment and with urolithin C for 10 min, n = 5. (c) A pancreas was perfused with 8.3 mmol·L^{-1} glucose before addition of urolithin C and then glucose concentration was reduced to 5 mmol·L^{-1}. (d) Histogram depicts the AUC of insulin release (from panel C) at different time ranges. There was a significant effect of the treatment. *P < .05, significantly different as indicated; one-way ANOVA with Holm–Sidak test, n = 5. The arrows indicate the time point of urolithin C addition (20 μmol·L^{-1})

model Ca_v channel Ca_vAb (Tang et al., 2016). Figure 6a shows the docked pose of urolithin C within the channel, and Figure 6b highlights the side chain of residues involved in the ligand-protein recognition. The analysis of the complex suggested that urolithin C forms three hydrogen bonds (for a schematic representation, see Figure 6c), one between Tyr1489 and the carbonyl group, one between Glu1144 and a hydroxyl group, and one between Glu393 and a hydroxyl group. Finally, a π-stacking interaction is expected between Phe1143 side chain ring and the mono-hydroxylated ring of urolithin C.

Secondly, the possible urolithin C-induced changes in intracellular Ca^{2+} ($[Ca^{2+}]_i$) in pancreatic beta cell was investigated (Figures 7 and S5). In INS-1 cells, the depolarizing agent KCl (15 mmol·L^{-1}) induced a fast $[Ca^{2+}]_i$ rise, as illustrated by the increase in F340/F380 Fura-2AM fluorescence ratio (Figure 7a). Urolithin C (20 μmol·L^{-1}) enhanced the KCl-induced $[Ca^{2+}]_i$ rise (Figure 7b,d); displaying no effect on $[Ca^{2+}]_i$ under basal condition (Figure 7c,d). Importantly, these observations were confirmed in dispersed cells isolated from rat islets in which 20 μmol·L^{-1} of urolithin C enhanced KCl-induced $[Ca^{2+}]_i$ increase (Figure S5A,B,D) and had no effect on $[Ca^{2+}]_i$ under basal condition (Figures S5C,D). Furthermore, in the presence of nimodipine, an L-type Ca^{2+} channel inhibitor (Alexander et al., 2017), the KCl-induced rise in $[Ca^{2+}]_i$ was reduced, validating Ca^{2+} channel blockade. Importantly, the enhancing effect of urolithin C on KCl-induced response was completely abolished in the presence of nimodipine (Figure 7d).

Finally, the ability of urolithin C to modulate the L-type Ca^{2+} current in INS-1 cells was investigated. In the whole-cell configuration of patch-clamp technique, with Ba^{2+} as the charge carrier, 20 μmol·L^{-1} of urolithin C increased the L-type Ba^{2+} current (Figure 8a,b). After the enhancement of the current by urolithin C, nimodipine treatment reduced it by 84.8 ± 2.6% (n = 5; Figure 8a). Moreover, currents

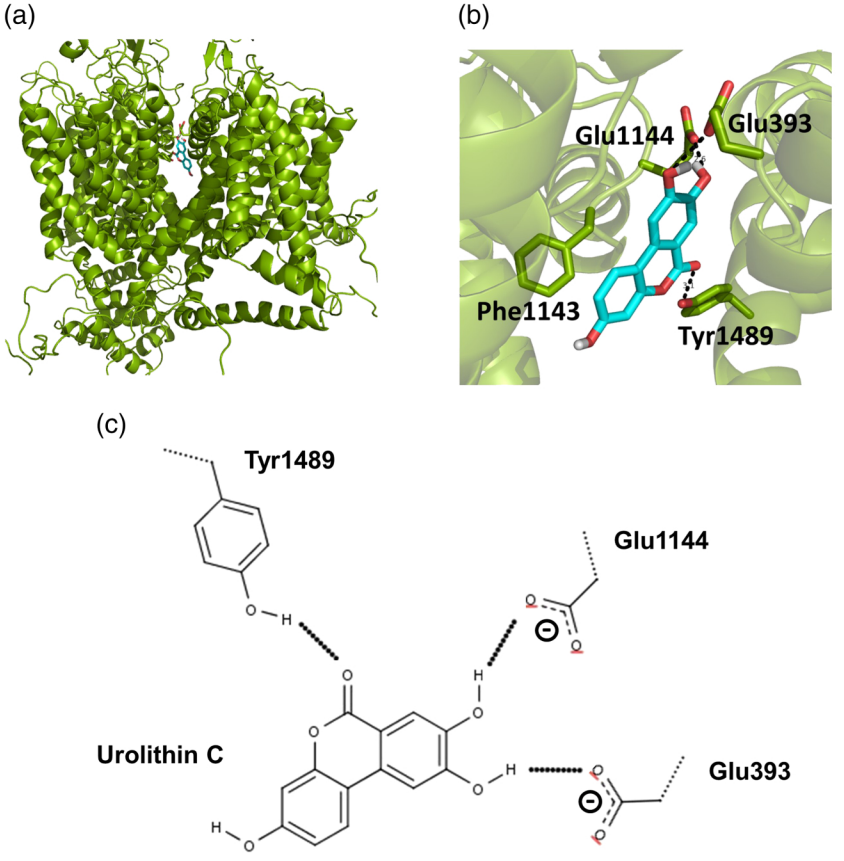

FIGURE 6 Docking of urolithin C at the $Ca_v1.2$ channel α1C subunit model. The $Ca_v1.2$ channel α1c subunit model and urolithin C are shown in green and cyan respectively. (a) Large view of urolithin C docked inside the $Ca_v1.2$ channel. (b) Zoom view of urolithin C docked inside the $Ca_v1.2$ channel showing the hydrogen bonding in black dash. (c) Schematic representation of the hydrogen bonding between urolithin C and the $Ca_v1.2$ channel

beforehand inhibited by nimodipine were weakly modulated by urolithin C (+ 4.0 ± 1.3%, n = 5, Figure S6). The effect of urolithin C on L-type current was concentration dependent and observed within the micromolar range (Figure 8c); it developed rapidly, reaching its maximum within 30 s after urolithin C perfusion and remaining stable thereafter (Figure 8d). This effect could be reversed after the removal of urolithin C (Figure S7). The enhancement of the L-type current by urolithin C was not the same for all voltage stimulation. Indeed, urolithin C-enhanced L-type Ba^{2+} current was greater for depolarization around −20 mV compared to lower and larger depolarizations, as illustrated by current–voltage relationship normalized to 1 for the maximum current (−10 mV; Figure 8e). Consequently, urolithin C induced a decrease of the potential at half-maximal activation ($V_{0.5}$) of the L-type current (from −17.9 ± 1.0 mV to −22.3 ± 1.0 mV, for control vs. urolithin C respectively; n = 5, P < .05; t-test). By contrast, 20 μmol·L^{-1} of urolithin C did not affect the rapidly inactivating T-type Ca^{2+} currents in INS-1 cells (Figure 8f). In summary, the mechanistic studies suggest that urolithin C modulates L-type Ca^{2+} channels, facilitating their opening, which in turn enhances Ca^{2+} influx.

4 | DISCUSSION

In the present study, we tested a set of several polyphenol metabolites for their activity on beta cell function with the aim of identifying compounds capable of enhancing glucose-stimulated insulin secretion. On this basis, urolithins A, B, C, and D were selected among 30 polyphenol metabolites and were further studied.

Urolithins are circulating polyphenol metabolites that originate from ellagitannins present in foods such as pomegranates, nuts, and berries. In a series of gut microbiota-mediated reactions, ellagitannins are hydrolysed yielding ellagic acid, which is converted to urolithins through the loss of one of its two lactones and by successive removal of hydroxyl groups (Espín et al., 2013). This process leads to the production of urolithin A, urolithin B, urolithin C, and urolithin D. Urolithins have been shown to regulate cellular processes involved in normal and pathological conditions (Espín et al., 2013; Kang, Kim, Tomás-Barberán, Espín, & Chung, 2016; Tang et al., 2017). A few recent studies have also reported that administration and consumption of these colonic metabolites, in particular urolithin A, promote positive health outcomes in animal models (Ryu et al., 2016; Savi et al., 2017; Tang et al., 2017). However and until now, the pharmacological effect of urolithins on endocrine pancreatic function has not been determined.

Most studies on the biological activities on urolithins have focused on urolithins A and B since these compounds and their derivatives were shown to be the main ellagitannin metabolites detected in humans with high variability across individuals (Espín et al., 2013; Tomás-Barberán, García-Villalba, González-Sarrías, Selma, & Espín, 2014). In the present work, we have not adopted a nutritionally based approach; instead, we concentrated on the spectrum of pharmacological properties of urolithins on beta cell function. This framework led

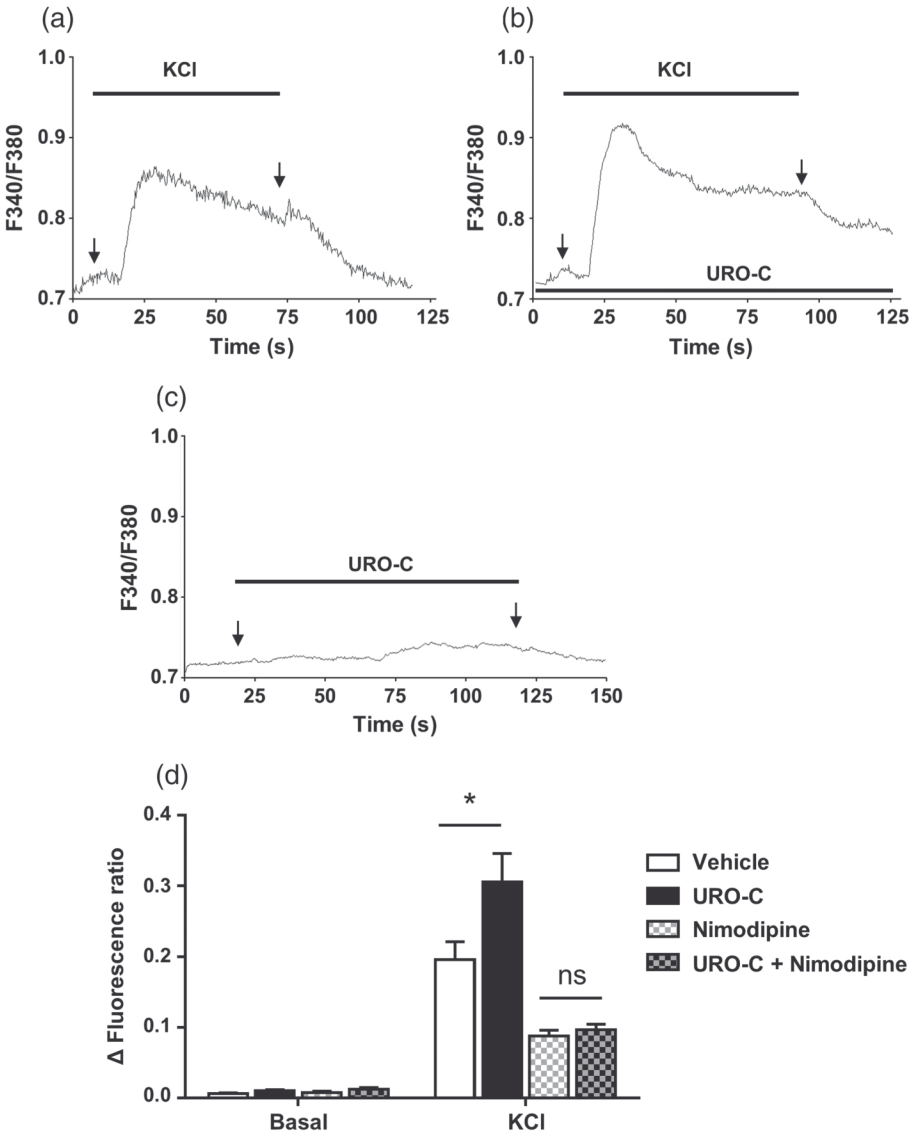

FIGURE 7 Effects of urolithin C on depolarisation-induced rise in intracellular calcium in INS-1 cells. $[Ca^{2+}]_i$ was monitored using the ratiometric fluorescent Ca^{2+} indicator Fura-2AM. INS-1 cells were incubated with 20 μmol·L^{-1} urolithin C in the absence or presence of 20 μmol·L^{-1} of nimodipine. Typical recordings illustrate variations of fluorescence ratio (F340/F380) and rise in $[Ca^{2+}]_i$ in response to 15 mmol·L^{-1} KCl in the absence (a) or presence of urolithin C (b) and in response to urolithin C under basal condition (c). (d) The histogram depicts the mean of the maximal variation in the fluorescence ratio. There was an effect of KCl and the treatment as well as an interaction between both factors. *P < .05, significantly different as indicated; ns, non-significant; two-way ANOVA with Holm–Sidak test; n = 6

us to focus on the less characterized urolithin C that we found to be particularly active to enhance insulin secretion induced by glucose both in normal and dysfunctional cells. The distinct pharmacological capacities of urolithins revealed here are in line with previous studies showing that urolithins C and D bind to the **ephrin type-A receptor 2** whereas urolithins A and B do not (Giorgio et al., 2015). Similarly, 50 μmol·L^{-1} of urolithins A and B are approximately twice more effective to extend the lifespan of *Caenorhabditis elegans* as compared to urolithin D (Ryu et al., 2016). Here, we report that micromolar concentrations of urolithin C were sufficient to enhance insulin secretion in different models. Such pharmacological concentrations (Wright, 2013) can be reached in rat plasma following i.p. administration of urolithin C (Bayle et al., 2016).

We found that, within the same range of concentration, urolithin C enhanced (a) glucose-induced insulin secretion in INS-1 cells, rat isolated islets, and isolated perfused pancreas, (b) depolarization-evoked rise in $[Ca^{2+}]_i$ both in INS-1 cells and in dispersed cells isolated from rat islets, and (c) L-type Ca^{2+} currents in INS-1 cells. The use of the L-type Ca^{2+} channel inhibitor nimodipine (Alexander et al., 2017) allowed us to identify $Ca_v1.x$ channels as key mediators of the pharmacological effect of urolithin C. This latter finding is particularly relevant as these channels, which mediate L-type currents, are thought to play a predominant role over the other types of Ca^{2+} channels to initiate insulin exocytosis from beta cells (Yang & Berggren, 2006). The effect on L-type Ca^{2+} current occurred within a few seconds, raising the possibility that urolithin C directly targeted $Ca_v1.x$ channels, notably the

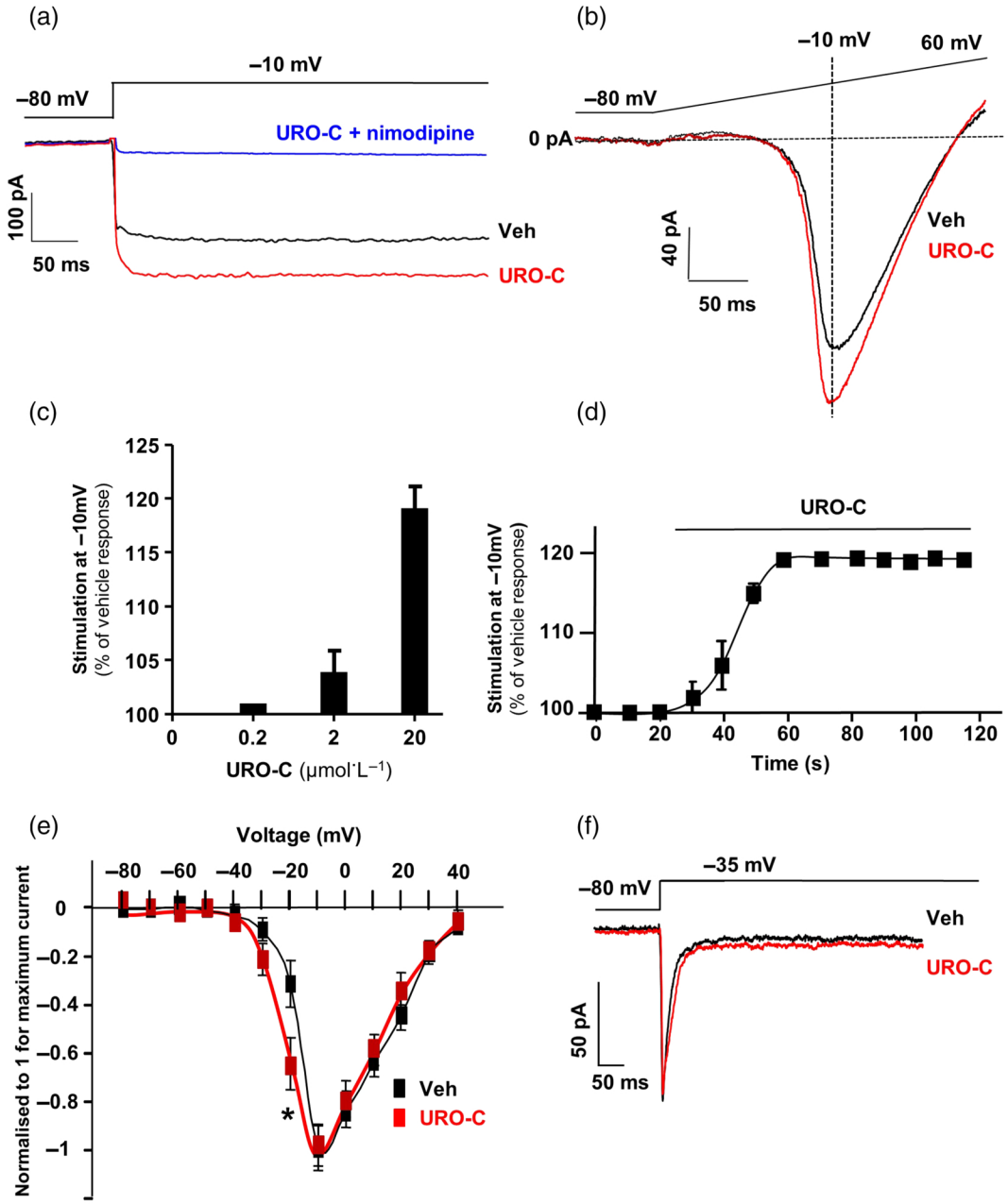

FIGURE 8 Effects of urolithin C on L- and T-type Ca^{2+} channel currents carried by Ba^{2+} in INS-1 cells. (a) Typical traces of slow inactivated L-type Ca^{2+} current in the absence (Veh), presence of 20 μmol·L^{-1} urolithin C (URO-C) or urolithin C + nimodipine (20 μmol·L^{-1}). (b) Typical traces of L-type Ca^{2+} current stimulated by a ramp depolarization in the absence (Veh) or presence of 20 μmol·L^{-1} urolithin C. (c) Concentration–response of urolithin C on the L-type current recorded at −10 mV. The histogram depicts the mean of current expressed as the percentage of current obtained in the presence of vehicle, n = 5. (d) Time course of the effect of 20 μmol·L^{-1} of urolithin C on L-type Ca^{2+} current (frequency of stimulation of 0.1 Hz, urolithin C was perfused at t = 20 s). The data represent the mean of current expressed as the percentage of current obtained in the presence of vehicle, n = 5. (e) Effect of 20 μmol·L^{-1} of urolithin C on the current-to-voltage (I/V) relationship of L-type current. Both curves were normalized to 1 (maximum current; holding potential −80 mV, depolarization steps of 10-mV increments at 0.1 Hz from −80 to 40 mV). For the negative potentials there was an effect of the treatment and an interaction between treatment and depolarization. *P < .05 significantly different from Veh at −20 mV, two-way ANOVA with Holm–Sidak test, n = 5. (f) Effect of 20 μmol·L^{-1} of urolithin C on typical T-type Ca^{2+} current

pore-forming subunit α1 (Catterall, 2011). Our docking simulation that predicts intermolecular interactions between urolithin C and several amino acids of the α1c subunit also supports this hypothesis. Of note, our data suggest that urolithin C forms hydrogen bound with Tyr1489, a residue whose mutation affects the voltage-dependent actions of dihydropyridine modulators (Bodi et al., 1997). Furthermore, the observation that urolithin C did not modulate T-type Ca^{2+} currents suggests a relative selectivity towards $Ca_v1.x$ channels.

Patch-clamp recordings also showed that urolithin C stimulated L-type current in a concentration- and voltage-dependent manner. Stimulation occurred at membrane potentials above depolarization threshold, with a higher effect between −40 and 0 mV, which resulted in a

decrease of the $V_{0.5}$. This is expected to enhance glucose-induced Ca^{2+} influx and thus insulin secretion in the presence of urolithin C. By contrast, urolithin C did not change the activation threshold of the calcium current and had no effect at resting membrane potential. This feature is in agreement with the finding that urolithin C was unable to trigger a rise in $[Ca^{2+}]_i$ in the absence of depolarization, notably under a non-stimulating glucose concentration (low resting membrane potential). It could also explain the effect of urolithin C on insulin secretion induced by a stimulating concentration of glucose or by glibenclamide, a drug known to induce membrane depolarization through closure of K_{ATP} channels (Tahrani, Barnett, & Bailey, 2016). This is also in agreement with the reversible action of urolithin C in isolated perfused pancreas since insulin release returned to baseline levels when glucose was reduced to a non-stimulating concentration even though urolithin C was still present. Taken as a whole, our mechanistic studies are compatible with a glucose-dependent regulation of insulin secretion by urolithin C.

Health benefits of polyphenols or their derivatives have been traditionally attributed to their antioxidant properties (Del Rio et al., 2013; Espín et al., 2013; Martel et al., 2017). Our studies suggest that urolithin C is not merely an antioxidant molecule but can possibly function as a pharmacological agent in pancreatic beta cells by regulating cell surface proteins and intracellular signalling pathways, as shown previously with a number of products generated by gut microbiota (Husted, Trauelsen, Rudenko, Hjorth, & Schwartz, 2017). This possibility could also apply to urolithin A, as it also exhibited some activity in INS-1 cells but further work is necessary to detail how this compound regulates beta cell function. Owing to the ubiquitous nature of Ca^{2+} which is a second messenger mediating a myriad of cellular processes, L-type Ca^{2+} channels serve a variety of vital functions including muscle contraction or neurotransmission (Catterall, 2011). Therefore, our findings are of potential interest for explaining other biological activities that have been attributed to urolithins in vitro and in vivo (Espín et al., 2013).

The pharmacological properties of urolithin C revealed here make it a potentially valuable compound to ameliorate beta cell function, especially to sustain insulin secretion when glucose concentration exceeds threshold. Such compounds are currently used to treat Type 2 diabetes in which beta cell dysfunction is a core feature of the disease (Vetere et al., 2014). We therefore ensured that urolithin C retains some efficiency in enhancing glucose-induced insulin secretion in INS-1 cells exposed to high glucose concentration, a cellular model used to mirror the deterioration of beta cell function due to glucotoxicity (Quinault et al., 2016). For the same purpose, the antioxidant activity of urolithin C may constitute an additional asset since beta cells and other cell types implicated in diabetes-related complications are particularly vulnerable to oxidative stress, stemming from metabolic dysregulation (Schwartz et al., 2017). The multi-target nature of urolithins as well as their effect on Ca^{2+} signalling, at least for urolithin C, may possibly raise some concerns regarding their low selectivity and potential toxicity and thus constitute a drawback for their use in vivo. Nevertheless, until now, in vivo administration of urolithins failed to demonstrate any safety concerns (Heilman, Andreux, Tran, Rinsch, & Blanco-Bose, 2017) but was rather found to exert a protective role and to ameliorate age-related conditions (Ryu et al., 2016; Savi et al., 2017; Tang et al., 2017).

In conclusion, our findings revealed that the microbiota ellagitannin metabolites urolithins A, B, C, and D differently modulate glucose- and glibenclamide-induced insulin secretion. Our data support the conclusion that one promising compound, urolithin C, exerts a rapid, sustained, reversible, and glucose-dependent effect on insulin secretion. Through the implementation of complementary approaches, we also provide a mechanistic understanding involving L-type Ca^{2+} channels in urolithin C bioactivity. Our work sheds light on a mechanism by which polyphenol metabolites exert pharmacological activities and constitutes a preliminary step towards the design of polyphenol metabolite-based or metabolite -inspired compounds to ameliorate beta cell function.

ACKNOWLEDGEMENTS

This work was supported in part by the SATT AxLR and the Agence Nationale de la Recherche under Grant ANR-10-BINF-03-03. We thank René Gross for technical assistance.

AUTHOR CONTRIBUTIONS

M.B., M.D.'A., G.G., and E.Y. performed insulin secretion experiments in INS-1 cells. M.B. performed insulin secretion experiments in isolated islets of Langerhans and perfused pancreas. A.V. performed intracellular calcium experiments. J.-F.Q. performed electrophysiological experiments. J.-F.G. performed docking simulation. M.B., M.D.'A., A.V., J.-F.Q., J.-F.G., J.N., C.O., G.C., and R.M. contributed to the design, analysis, and interpretation of the data. G.C., R.M., J.N., and C.O. wrote the manuscript; D.D.R. and A.C. made critical comments on the manuscript. G.C., C.O., R.M., D.D.R., and A.C. initiated the project. G.C., C.O., R.M. managed the project. All authors approved the final version to be published.

CONFLICT OF INTEREST

The authors declare no conflicts of interest.

DECLARATION OF TRANSPARENCY AND SCIENTIFIC RIGOUR

This Declaration acknowledges that this paper adheres to the principles for transparent reporting and scientific rigour of preclinical research as stated in the *BJP* guidelines for Design & Analysis, and Animal Experimentation, and as recommended by funding agencies, publishers and other organisations engaged with supporting research.

REFERENCES

Alexander, S. P. H., Fabbro, D., Kelly, E., Marrion, N. V., Peters, J. A., Faccenda, E., … Collaborators, C. G. T. P. (2017). The Concise Guide to PHARMACOLOGY 2017/18: Catalytic receptors. *British Journal of Pharmacology*, *174*, S225–S271. https://doi.org/10.1111/bph.13876

Alexander, S. P. H., Striessnig, J., Kelly, E., Marrion, N. V., Peters, J. A., Faccenda, E., … CGTP Collaborators (2017). The Concise Guide to PHARMACOLOGY 2017/18: Voltage-gated ion channels: THE CONCISE GUIDE TO PHARMACOLOGY 2017/18: Voltage-gated ion channels. *British Journal of Pharmacology*, *174*, S160–S194. https://doi.org/10.1111/bph.13884

Bai, X., Yang, P., Zhou, Q., Cai, B., Buist-Homan, M., Cheng, H., … Shi, G. (2017). The protective effect of the natural compound hesperetin against fulminant hepatitis in vivo and in vitro. *British Journal of Pharmacology*, *174*, 41–56. https://doi.org/10.1111/bph.13645

Bardy, G., Virsolvy, A., Quignard, J. F., Ravier, M. A., Bertrand, G., Dalle, S., … Oiry, C. (2013). Quercetin induces insulin secretion by direct activation of L-type calcium channels in pancreatic beta cells. *British Journal of Pharmacology*, *169*, 1102–1113. https://doi.org/10.1111/bph.12194

Bayle, M., Roques, C., Marion, B., Audran, M., Oiry, C., Bressolle-Gomeni, F. M. M., & Cros, G. (2016). Development and validation of a liquid chromatography-electrospray ionization-tandem mass spectrometry method for the determination of urolithin C in rat plasma and its application to a pharmacokinetic study. *Journal of Pharmaceutical and Biomedical Analysis*, *131*, 33–39. https://doi.org/10.1016/j.jpba.2016.07.046

Bodi, I., Yamaguchi, H., Hara, M., He, M., Schwartz, A., & Varadi, G. (1997). Molecular studies on the voltage dependence of dihydropyridine action on L-type Ca $^{2+}$ channels: CRITICAL INVOLVEMENT OF TYROSINE RESIDUES IN MOTIF IIIS6 AND IVS6. *The Journal of Biological Chemistry*, *272*, 24952–24960. https://doi.org/10.1074/jbc.272.40.24952

Broca, C., Quoyer, J., Costes, S., Linck, N., Varrault, A., Deffayet, P.-M., … Bertrand, G. (2009). β-Arrestin 1 is required for PAC_1 receptor-mediated potentiation of long-lasting ERK1/2 activation by glucose in pancreatic β-cells. *Journal of Biological Chemistry*, *284*, 4332–4342. https://doi.org/10.1074/jbc.M807595200

Catterall, W. A. (2011). Voltage-gated calcium channels. *Cold Spring Harbor Perspectives in Biology*, *3*, a003947.

Curtis, M. J., Alexander, S., Cirino, G., Docherty, J. R., George, C. H., Giembycz, M. A., … Ahluwalia, A. (2018). Experimental design and analysis and their reporting II: Updated and simplified guidance for authors and peer reviewers. *British Journal of Pharmacology*, *175*, 987–993. https://doi.org/10.1111/bph.14153

Dall'Asta, M., Bayle, M., Neasta, J., Scazzina, F., Bruni, R., Cros, G., … Oiry, C. (2015). Protection of pancreatic β-cell function by dietary polyphenols. *Phytochemistry Reviews*, *14*, 933–959. https://doi.org/10.1007/s11101-015-9429-x

Del Rio, D., Rodriguez-Mateos, A., Spencer, J. P. E., Tognolini, M., Borges, G., & Crozier, A. (2013). Dietary (poly)phenolics in human health: Structures, bioavailability, and evidence of protective effects against chronic diseases. *Antioxidants & Redox Signaling*, *18*, 1818–1892.

Espín, J. C., Larrosa, M., García-Conesa, M. T., & Tomás-Barberán, F. (2013). Biological significance of urolithins, the gut microbial ellagic Acid-derived metabolites: The evidence so far. *Evidence-Based Complementary and Alternative Medicine*, *2013*, 270418.

Fusi, F., Spiga, O., Trezza, A., Sgaragli, G., & Saponara, S. (2017). The surge of flavonoids as novel, fine regulators of cardiovascular Cav channels. *European Journal of Pharmacology*, *796*, 158–174. https://doi.org/10.1016/j.ejphar.2016.12.033

Giorgio, C., Mena, P., Del Rio, D., Brighenti, F., Barocelli, E., Hassan-Mohamed, I., … Tognolini, M. (2015). The ellagitannin colonic metabolite urolithin D selectively inhibits EphA2 phosphorylation in prostate cancer cells. *Molecular Nutrition & Food Research*, *59*, 2155–2167. https://doi.org/10.1002/mnfr.201500470

Goszcz, K., Duthie, G. G., Stewart, D., Leslie, S. J., & Megson, I. L. (2017). Bioactive polyphenols and cardiovascular disease: Chemical antagonists, pharmacological agents or xenobiotics that drive an adaptive response? *British Journal of Pharmacology*, *174*, 1209–1225. https://doi.org/10.1111/bph.13708

Gross, R., Roye, M., Manteghetti, M., Hillaire-Buys, D., & Ribes, G. (1995). Alterations of insulin response to different beta cell secretagogues and pancreatic vascular resistance induced by N omega-nitro-L-arginine methyl ester. *British Journal of Pharmacology*, *116*, 1965–1972. https://doi.org/10.1111/j.1476-5381.1995.tb16399.x

Gu, M., Zhang, Y., Liu, C., Wang, D., Feng, L., Fan, S., … Huang, C. (2017). Morin, a novel liver X receptor α/β dual antagonist, has potent therapeutic efficacy for nonalcoholic fatty liver diseases. *British Journal of Pharmacology*, *174*, 3032–3044. https://doi.org/10.1111/bph.13933

Harding, S. D., Sharman, J. L., Faccenda, E., Southan, C., Pawson, A. J., Ireland, S., … NC-IUPHAR (2018). The IUPHAR/BPS Guide to PHARMACOLOGY in 2018: Updates and expansion to encompass the new guide to IMMUNOPHARMACOLOGY. *Nucleic Acids Research*, *46*, D1091–D1106. https://doi.org/10.1093/nar/gkx1121

Heilman, J., Andreux, P., Tran, N., Rinsch, C., & Blanco-Bose, W. (2017). Safety assessment of Urolithin A, a metabolite produced by the human gut microbiota upon dietary intake of plant derived ellagitannins and ellagic acid. *Food and Chemical Toxicology*, *108*, 289–297. https://doi.org/10.1016/j.fct.2017.07.050

Husted, A. S., Trauelsen, M., Rudenko, O., Hjorth, S. A., & Schwartz, T. W. (2017). GPCR-Mediated Signaling of Metabolites. *Cell Metabolism*, *25*, 777–796.

Jamen, F., Puech, R., Bockaert, J., Brabet, P., & Bertrand, G. (2002). Pituitary adenylate cyclase-activating polypeptide receptors mediating insulin secretion in rodent pancreatic islets are coupled to adenylate cyclase but not to PLC. *Endocrinology*, *143*, 1253–1259. https://doi.org/10.1210/endo.143.4.8739

Kang, I., Kim, Y., Tomás-Barberán, F. A., Espín, J. C., & Chung, S. (2016). Urolithin A, C, and D, but not iso-urolithin A and urolithin B, attenuate triglyceride accumulation in human cultures of adipocytes and hepatocytes. *Molecular Nutrition & Food Research*, *60*, 1129–1138. https://doi.org/10.1002/mnfr.201500796

Kilkenny, C., Browne, W., Cuthill, I. C., Emerson, M., & Altman, D. G. (2010). Animal research: Reporting *in vivo* experiments: the ARRIVE guidelines. *British Journal of Pharmacology*, *160*, 1577–1579.

Martel, J., Ojcius, D. M., Chang, C.-J., Lin, C.-S., Lu, C.-C., Ko, Y.-F., … Young, J. D. (2017). Anti-obesogenic and antidiabetic effects of plants and mushrooms. *Nature Reviews. Endocrinology*, *13*, 149–160. https://doi.org/10.1038/nrendo.2016.142

Miteva, M. A., Guyon, F., & Tufféry, P. (2010). Frog2: Efficient 3D conformation ensemble generator for small compounds. *Nucleic Acids Research*, *38*, W622–W627. https://doi.org/10.1093/nar/gkq325

Oak, M.-H., Auger, C., Belcastro, E., Park, S.-H., Lee, H.-H., & Schini-Kerth, V. B. (2018). Potential mechanisms underlying cardiovascular protection by polyphenols: Role of the endothelium. *Free Radical Biology & Medicine*, *122*, 161–170. https://doi.org/10.1016/j.freeradbiomed.2018.03.018

Oh, D. Y., & Olefsky, J. M. (2016). G protein-coupled receptors as targets for anti-diabetic therapeutics. *Nature Reviews. Drug Discovery*, *15*, 161–172. https://doi.org/10.1038/nrd.2015.4

Peyot, M.-L., Gray, J. P., Lamontagne, J., Smith, P. J. S., Holz, G. G., Madiraju, S. R. M., … Heart, E. (2009). Glucagon-like peptide-1 induced signaling and insulin secretion do not drive fuel and energy metabolism in primary rodent pancreatic β-cells. *PLoS ONE*, *4*, e6221. https://doi.org/10.1371/journal.pone.0006221

Pihan, E., Colliandre, L., Guichou, J.-F., & Douguet, D. (2012). e-Drug3D: 3D structure collections dedicated to drug repurposing and fragment-based drug design. *Bioinformatics*, *28*, 1540–1541. https://doi.org/10.1093/bioinformatics/bts186

Pons, J.-L., & Labesse, G. (2009). @TOME-2: A new pipeline for comparative modeling of protein-ligand complexes. *Nucleic Acids Research*, *37*, W485–W491. https://doi.org/10.1093/nar/gkp368

Quinault, A., Gausseres, B., Bailbe, D., Chebbah, N., Portha, B., Movassat, J., & Tourrel-Cuzin, C. (2016). Disrupted dynamics of F-actin and insulin granule fusion in INS-1 832/13 beta-cells exposed to glucotoxicity: partial restoration by glucagon-like peptide 1. *Biochimica et Biophysica Acta (BBA) - Molecular Basis of Disease*, *1862*, 1401–1411. https://doi.org/10.1016/j.bbadis.2016.04.007

Rebuffat, S. A., Sidot, E., Guzman, C., Azay-Milhau, J., Jover, B., Lajoix, A.-D., & Peraldi-Roux, S. (2018). Adipose tissue derived-factors impaired pancreatic β-cell function in diabetes. *Biochimica et Biophysica Acta (BBA) - Molecular Basis of Disease*, *1864*, 3378–3387. https://doi.org/10.1016/j.bbadis.2018.07.024

Rodriguez-Mateos, A., Vauzour, D., Krueger, C. G., Shanmuganayagam, D., Reed, J., Calani, L., … Crozier, A. (2014). Bioavailability, bioactivity and impact on health of dietary flavonoids and related compounds: An update. *Archives of Toxicology*, *88*, 1803–1853. https://doi.org/10.1007/s00204-014-1330-7

Rorsman, P., & Ashcroft, F. M. (2018). Pancreatic β-cell electrical activity and insulin secretion: Of mice and men. *Physiological Reviews*, *98*, 117–214. https://doi.org/10.1152/physrev.00008.2017

Ryu, D., Mouchiroud, L., Andreux, P. A., Katsyuba, E., Moullan, N., Nicolet-Dit-Félix, A. A., … Auwerx, J. (2016). Urolithin A induces mitophagy and prolongs lifespan in C. *elegans* and increases muscle function in rodents. *Nature Medicine*, *22*, 879–888. https://doi.org/10.1038/nm.4132

Saponara, S., Carosati, E., Mugnai, P., Sgaragli, G., & Fusi, F. (2011). The flavonoid scaffold as a template for the design of modulators of the vascular $Ca_v1.2$ channels. *British Journal of Pharmacology*, *164*, 1684–1697. https://doi.org/10.1111/j.1476-5381.2011.01476.x

Savi, M., Bocchi, L., Mena, P., Dall'Asta, M., Crozier, A., Brighenti, F., … Del Rio, D. (2017). In vivo administration of urolithin A and B prevents the occurrence of cardiac dysfunction in streptozotocin-induced diabetic rats. *Cardiovascular Diabetology*, *16*, 80. https://doi.org/10.1186/s12933-017-0561-3

Schwartz, S. S., Epstein, S., Corkey, B. E., Grant, S. F. A., Gavin Iii, J. R., Aguilar, R. B., & Herman, M. E. (2017). A unified pathophysiological construct of diabetes and its complications. *Trends in Endocrinology and Metabolism*, *28*, 645–655. https://doi.org/10.1016/j.tem.2017.05.005

Stalmach, A., Mullen, W., Barron, D., Uchida, K., Yokota, T., Cavin, C., … Crozier, A. (2009). Metabolite profiling of hydroxycinnamate derivatives in plasma and urine after the ingestion of coffee by humans: Identification of biomarkers of coffee consumption. *Drug Metabolism and Disposition*, *37*, 1749–1758. https://doi.org/10.1124/dmd.109.028019

Tahrani, A. A., Barnett, A. H., & Bailey, C. J. (2016). Pharmacology and therapeutic implications of current drugs for type 2 diabetes mellitus. *Nature Reviews. Endocrinology*, *12*, 566–592. https://doi.org/10.1038/nrendo.2016.86

Tang, L., Gamal El-Din, T. M., Swanson, T. M., Pryde, D. C., Scheuer, T., Zheng, N., & Catterall, W. A. (2016). Structural basis for inhibition of a voltage-gated Ca^{2+} channel by Ca^{2+} antagonist drugs. *Nature*, *537*, 117–121. https://doi.org/10.1038/nature19102

Tang, L., Mo, Y., Li, Y., Zhong, Y., He, S., Zhang, Y., … Chen, A. (2017). Urolithin A alleviates myocardial ischemia/reperfusion injury via PI3K/Akt pathway. *Biochemical and Biophysical Research Communications*, *486*, 774–780. https://doi.org/10.1016/j.bbrc.2017.3.119

Tognolini, M., Giorgio, C., Hassan Mohamed, I., Barocelli, E., Calani, L., Reynaud, E., … del Rio, D. (2012). Perturbation of the EphA2–EphrinA1 system in human prostate cancer cells by colonic (poly)phenol catabolites. *Journal of Agricultural and Food Chemistry*, *60*, 8877–8884. https://doi.org/10.1021/jf205305m

Tomás-Barberán, F. A., García-Villalba, R., González-Sarrías, A., Selma, M. V., & Espín, J. C. (2014). Ellagic acid metabolism by human gut microbiota: consistent observation of three urolithin phenotypes in intervention trials, independent of food source, age, and health status. *Journal of Agricultural and Food Chemistry*, *62*, 6535–6538. https://doi.org/10.1021/jf5024615

Vetere, A., Choudhary, A., Burns, S. M., & Wagner, B. K. (2014). Targeting the pancreatic β-cell to treat diabetes. *Nature Reviews. Drug Discovery*, *13*, 278–289. https://doi.org/10.1038/nrd4231

Webb, B., & Sali, A. (2017). Protein Structure Modeling with MODELLER. *Methods in Molecular Biology*, *1654*, 39–54. https://doi.org/10.1007/978-1-4939-7231-9_4

Williamson, G., Kay, C. D., & Crozier, A. (2018). The bioavailability, transport, and bioactivity of dietary flavonoids: A review from a historical perspective. *Comprehensive Reviews in Food Science and Food Safety*, *17*, 1054–1112. https://doi.org/10.1111/1541-4337.12351

Wright, B. (2013). Forging a modern generation of polyphenol-based therapeutics. *British Journal of Pharmacology*, *169*, 844–847. https://doi.org/10.1111/bph.12195

Yang, S.-N., & Berggren, P.-O. (2006). The role of voltage-gated calcium channels in pancreatic β-cell physiology and pathophysiology. *Endocrine Reviews*, *27*, 621–676. https://doi.org/10.1210/er.2005-0888

Youl, E., Bardy, G., Magous, R., Cros, G., Sejalon, F., Virsolvy, A., … Oiry, C. (2010). Quercetin potentiates insulin secretion and protects INS-1 pancreatic β-cells against oxidative damage via the ERK1/2 pathway. *British Journal of Pharmacology*, *161*, 799–814. https://doi.org/10.1111/j.1476-5381.2010.00910.x

Youl, E., Magous, R., Cros, G., & Oiry, C. (2014). MAP Kinase cross talks in oxidative stress-induced impairment of insulin secretion. Involvement in the protective activity of quercetin. *Fundamental & Clinical Pharmacology*, *28*, 608–615. https://doi.org/10.1111/fcp.12078

Zhao, M., Ko, S.-Y., Garrett, I. R., Mundy, G. R., Gutierrez, G. E., & Edwards, J. R. (2018). The polyphenol resveratrol promotes skeletal growth in mice through a sirtuin 1-bone morphogenic protein 2 longevity axis. *British Journal of Pharmacology*, *175*, 4183–4192. https://doi.org/10.1111/bph.14477

Zheng, Y., Ley, S. H., & Hu, F. B. (2018). Global aetiology and epidemiology of type 2 diabetes mellitus and its complications. *Nature Reviews. Endocrinology*, *14*, 88–98. https://doi.org/10.1038/nrendo.2017.151